Available online at www.sciencedirect.com
SCIENCE DIRECT®
ELSEVIER
Journal of Sound and Vibration 291 (2006) 749–763
JOURNAL OF SOUND AND VIBRATION
www.elsevier.com/locate/jsvi

Improving active noise control in resonant fields

Jing Yuan*

Department of Mechanical Engineering, The Hong Kong Polytechnic University, Hunghom, Kowloon, Hong Kong

Received 6 September 2004; received in revised form 16 June 2005; accepted 25 June 2005
Available online 31 August 2005

Abstract

In active noise control (ANC), there is still room for further improvement in at least two directions: (1) how to use a finite impulse response (FIR) filter to suppress noise in a resonant field with infinite impulse response (IIR) paths; and (2) how to deal with non-minimum-phase (NMP) secondary paths. A new ANC configuration is proposed here. If the secondary path is minimum phase (MP), the new configuration is able to cancel broadband noise completely with a FIR filter. The same objective can only be achieved if one applies an IIR filter in an available ANC configuration. If the secondary path is NMP, the new configuration is able to minimize the H_2 norm of the noise path with a FIR filter. Again, this result can only be achieved if one applies an IIR filter in an available ANC configuration. Analytical and experimental results are given to demonstrate the significant improvement in almost the entire frequency range of interest.

1. Introduction

Active noise control (ANC) is an effective technique to suppress low-frequency noise [1,2]. Different feedback and feedforward control strategies are applied to ANC systems [3–5]. A possible application of ANC is the suppression of noise in resonant fields where path transfer functions have infinite impulse responses (IIR). To avoid the near-field effects, actuators and sensors in an ANC system may not be collocated and transfer functions between actuators and

*Tel.: +852 2766 7822; fax: +852 2365 4703.
E-mail address: mmjyuan@polyu.edu.hk.

0022-460X/$ - see front matter
doi:10.1016/j.jsv.2005.06.036

sensors are usually non-minimum-phase (NMP). These two problems affect ANC performance. A new method is proposed here to deal with these problems.

For ANC applications in resonant fields, the ideal transfer functions of controllers are IIR filters. Different adaptive algorithms were proposed to implement adaptive IIR filters for ANC applications [6–8]. For those adaptive IIR filters, there is a lack of stability guarantee in every step of adaptations. Recently, the adaptive lattice filters were introduced to solve the problem [9]. Despite the improvement in stability, adaptive IIR filters converge much slower than adaptive finite impulse response (FIR) filters. The stationary points of adaptive IIR filters could be local minima instead of global minima. It is recommended to use adaptive FIR filters whenever possible [10]. In this paper, a new ANC configuration is proposed in which an adaptive FIR filter is applied to minimize the H_2 norm of the noise path. To achieve the same result, an IIR filter must be applied in an available ANC configuration. Detailed explanations will be presented to show the differences between the new method and the available methods, as well as the advantages of the new method.

A transfer function F(z) is NMP if one or more of its zeros locate on or outside a unit circle centered at the origin of the complex z-plane. These zeros are known as NMP zeros. Since the NMP zeros of $F(z)$ are the NMP poles of $F^{-1}(z)$, an ideal ANC controller is unstable if part of its transfer function is the inverse of an NMP transfer function. In that case, a stable transfer function has to be substituted for the ideal yet unstable controller transfer function. This is a frequently encountered problem in many ANC applications.

Consider the ANC system in Fig. 1, where $P(z)$, $S(z)$, $R(z)$ and $F(z)$ denote the primary, secondary, reference and feedback transfer functions, respectively. It is assumed that these models match the respective physical paths with negligible errors. The gray-box in Fig. 1 represents an ANC controller $C(z) = (G(z))/\left(1 + \hat{F}(z)G(z)\right)$, in which signal-processing operations are carried out in internal blocks $\hat{F}(z)$ and $G(z)$, respectively. The objective of $\hat{F}(z)$ is to cancel the acoustical feedback path $F(z)$ in the noise field. If the model errors in $\hat{F}(z)$ are small enough, the closed-loop system is stable [1,2]. Here it is assumed that $\hat{F}(z) = F(z)$ to avoid unnecessary distractions. One may apply the block diagram algebra to Fig. 1 and obtain

$$
\begin{aligned}
e(z) &= \{P(z) + S(z)C(z)[I - F(z)C(z)]^{-1}R(z)\}n(z) \\
&= [P(z) + S(z)G(z)R(z)]n(z),
\end{aligned}
\tag{1}
$$

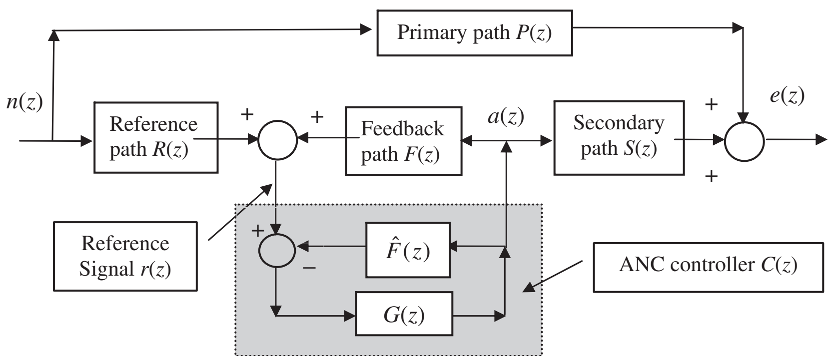

Fig. 1. Block diagram of an ANC system.

where $e(z)$ and $n(z)$ are, respectively, z-transforms of the error and primary source signals. An exact solution of $e(z)=0$ implies $G(z)=G_{\mathrm{id}}(z)=-S^{-1}(z)P(z)R^{-1}(z)$. This is the ideal controller to achieve $e(z)=0$ when the primary source is broadband white noise. One should find two problems in Eq. (1): (i) $G_{\mathrm{id}}(z)$ is an IIR filter even if $P(z)$, $S(z)$ and $R(z)$ are FIR filters; and (ii) $G_{\mathrm{id}}(z)$ is unstable if either $S(z)$ or $R(z)$ is NMP. For ANC applications in resonant noise fields, $P(z)$, $S(z)$ and $R(z)$ are IIR filters, and the expression of $G_{\mathrm{id}}(z)$ is more complicated but still contains $S^{-1}(z)$ and $R^{-1}(z)$. It is important to solve or approximate $\|P(z)+S(z)G(z)R(z)\|=0$ for ANC systems. Exact solutions have been reported requiring extra secondary sources [11,12] or extra sensors [13].

For a single-input and single-output (SISO) ANC system, there is no stable and exact solution of $||P(z)+S(z)G(z)R(z)||=0$ if $S(z)$ is NMP [11]. A minimum H_2 norm controller was proposed in Ref. [14], which is based on the exact knowledge of $P(z)$, $S(z)$ and direct availability of $n(z)$. In many applications, the primary noise does not come from a single source or the location of the primary source is uncertain. It may not be possible to obtain an accurate $P(z)$ in these applications. Besides, a reference signal must be measured to recover $n(z)$. A new method is proposed here to design and implement an adaptive H_2 controller without the knowledge of $P(z)$. This controller achieves the best performance by minimizing the H_2 norm of the noise path. Experimental results will be presented to verify the analysis results.

2. Dealing with IIR paths

For ANC systems in resonant sound fields, path models are best represented by IIR filters

$$P(z)=\frac{B_p(z)}{A(z)},\quad S(z)=\frac{B_s(z)}{A(z)},\quad R(z)=\frac{B_r(z)}{A(z)}\quad \text{and}\quad F(z)=\frac{B_f(z)}{A(z)}$$

with the same denominator $A(z)$. A common denominator shared by all path transfer functions in a system is the feature of a large class of distributed-parameter systems to which the modal theory is applicable [11]. Acoustical systems belong to this class. If $A(z)=1$, then all path models become FIR filters. Therefore, the proposed ANC structure is also applicable to other ANC applications if one sets $A(z)=1$ in the proposed ANC structure.

In this section, it is temporarily assumed that $S(z)$ and $R(z)$ are MP. A possible ANC structure is represented by the gray-box in Fig. 2. Although the gray-boxes in Figs. 1 and 2 have different structures, these controllers can be equivalent under a certain condition. A significant difference will be revealed at the end of this section to demonstrate an important advantage of the new ANC structure. One may apply the block diagram algebra to the gray-box of Fig. 2. The transfer function of this box can be derived as

$$C_{\mathrm{id}}(z)=\frac{-B_p(z)A(z)/B_s(z)B_r(z)}{1-B_p(z)B_f(z)/B_s(z)B_r(z)}=\frac{-B_p(z)A(z)}{B_s(z)B_r(z)-B_p(z)B_f(z)}. \tag{2}$$

The gray-boxes in Figs. 1 and 2 are equivalent to each other if internal block $G(z)$ of Fig. 1 is chosen to be

$$G_{\mathrm{id}}(z)=\frac{C_{\mathrm{id}}(z)}{1-F(z)C_{\mathrm{id}}(z)}.$$

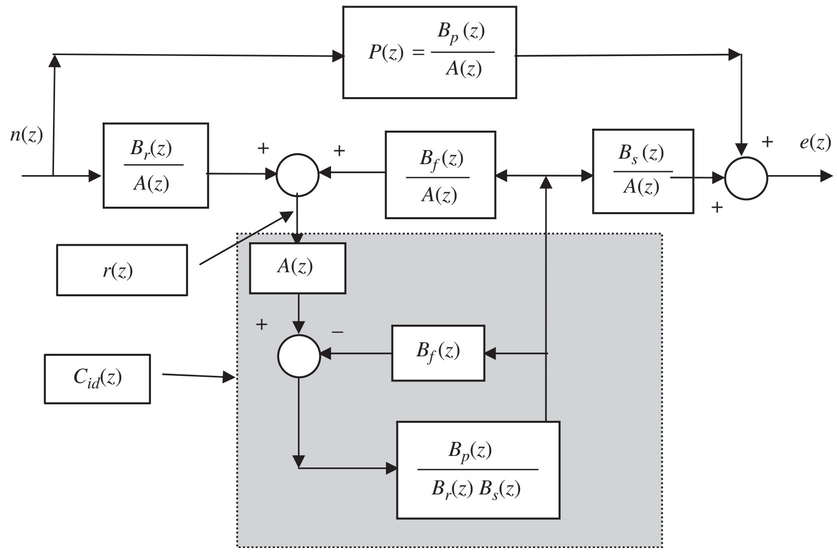

Fig. 2. Block diagram of the proposed ANC structure.

Substituting Eq. (2) into the equivalence condition, one can write

$$G_{\mathrm{id}}(z) = \frac{C_{\mathrm{id}}(z)}{1 - F(z)C_{\mathrm{id}}(z)} = \frac{-B_p(z)A(z)}{B_s(z)B_r(z)}. \tag{3}$$

If one further substitutes Eq. (3) and all the path transfer functions into Eq. (1), the result will be

$$e(z) = \left[\frac{B_p(z)}{A(z)} - \frac{B_s(z)B_p(z)B_r(z)}{A(z)B_s(z)B_r(z)}\right]n(z) = 0, \tag{4}$$

where $B_s(z)$ and $B_r(z)$ appear in the numerator and the denominator. Since $S(z)$ and $R(z)$ are MP by the temporary assumption in this section, $B_s(z)$ and $B_r(z)$ are MP polynomials whose effects are cancelled out such that $e(z) = 0$.

Therefore, for cancellation of broadband white noise, the ideal ANC controller may be implemented in two alternative and equivalent structures. One is represented by the gray-box of Fig. 2, whose transfer function is $C_{\mathrm{id}}(z)$ in Eq. (2). The other is represented by the gray-box of Fig. 1, with an internal block $G_{\mathrm{id}}(z)$ given by Eq. (3). Both $C_{\mathrm{id}}(z)$ and $G_{\mathrm{id}}(z)$ are IIR filters even if all path models become FIR filters when $A(z) = 1$. If either $C_{\mathrm{id}}(z)$ or $G_{\mathrm{id}}(z)$ is substituted by a FIR filter, it is analytically impossible to achieve $e(z) = 0$. This is a problem to be improved by the new ANC structures in Figs. 2 and 3.

In many applications, $P(z)$ is not available and Eq. (2) cannot be used to obtain the parameters of $C_{\mathrm{id}}(z)$ directly. Instead, the secondary path model $S(z)$ is used to obtain the filtered-x signal for online adaptation of controller $C(z)$ [1,2]. For the proposed ANC controller in Fig. 3, only numerator $B_c(z)$ is adaptive. All signal-processing operations in Fig. 3 are described mathematically by Eqs. (5)–(8). These operations are analyzed in the following part.

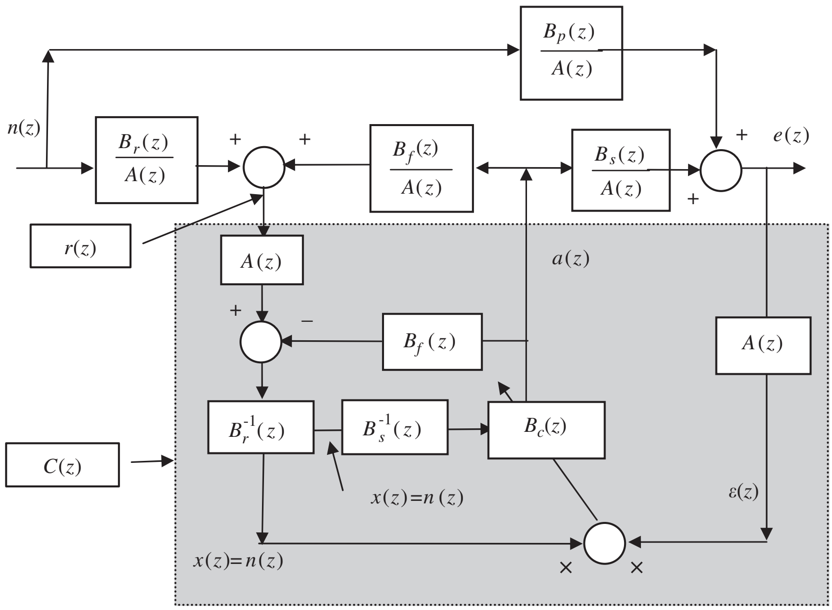

Fig. 3. Block diagram of the proposed ANC (adaptive).

The reference signal, given by

$$r(z) = \frac{B_r(z)}{A(z)}n(z) + \frac{B_f(z)}{A(z)}a(z),$$

is contributed by the primary and secondary sources. This signal is filtered by $A(z)$ and added to an internal signal $-B_f(z)a(z)$ to cancel the acoustical feedback. The resultant is then filtered by $B_r^{-1}(z)$ to be

$$\begin{aligned} x(z) &= \frac{1}{B_r(z)}\{A(z)r(z) - B_f(z)a(z)\} \\ &= \frac{1}{B_r(z)}\left\{A(z)\left[\frac{B_r(z)}{A(z)}n(z) + \frac{B_f(z)}{A(z)}a(z)\right] - B_f(z)a(z)\right\} = n(z). \end{aligned} \tag{5}$$

The coherence between $x(z)$ and $n(z)$ is an important problem in ANC systems. As long as $B_r(z)$ remains MP, a stable signal $x(z) = n(z)$ is recoverable by Eq. (5). This is practically possible if the reference sensor is sufficiently close to the primary source in our experiments. The actuation signal $a(z)$ is then synthesized from $x(z) = n(z)$ by

$$a(z) = \frac{B_c(z)}{B_s(z)}n(z). \tag{6}$$

Since $S(z)$, $F(z)$ and $R(z)$ are available with sufficient accuracy, as assumed by many ANC researchers, $A(z)$, $B_s(z)$, $B_r(z)$ and $B_f(z)$ are available with sufficient accuracy. Only $B_c(z)$ is not determined yet. It is adaptive in order to cancel an unknown FIR transfer function to be explained in due course. This is different from the available methods that use an adaptive FIR filter to approximate an IIR filter like $C_{id}(z)$ or $G_{id}(z)$.

To see the cancellation target of $B_c(z)$, one needs to examine the error signal, which is measured as

$$e(z) = \frac{B_p(z)}{A(z)} n(z) + \frac{B_s(z)}{A(z)} a(z).$$

Let $\varepsilon(z) = A(z)e(z)$, then one can write

$$\varepsilon(z) = B_p(z)n(z) + B_s(z)a(z) = \left[B_p(z) + B_c(z)\right] n(z), \tag{7}$$

upon substitution of Eq. (6) for $a(z)$. When $P(z)$ is not available, $B_p(z)$ is an unknown FIR filter whose effects should be cancelled by the application of adaptive FIR filter $B_c(z)$. Let $\{b_{pk}\}_{k=0}^{m}$ and $\{b_{ck}\}_{k=0}^{m}$ denote, respectively, coefficients of $B_p(z)$ and $B_c(z)$. One may express Eq. (7) in the time-domain as

$$\varepsilon(t) = \sum_{k=0}^{m} (b_{pk} + b_{ck}) n(t-k). \tag{8}$$

From Eq. (8), one can derive

$$\frac{\partial}{\partial b_{ck}} E\left\{\varepsilon^2(t)\right\} = 2E\left\{\varepsilon(t)n(t-k)\right\}.$$

The gradient vector of $E\{\varepsilon^2(t)\}$ consists of products of delayed samples of $x(t) = n(t)$ with the error signal $\varepsilon(t)$. The gray-box of Fig. 3 is based on the gray-box of Fig. 2 with additional operations to obtain the gradient vector given in Eq. (8).

In view of Eq. (7), the global minimum of $E\{\varepsilon^2(t)\} = 0$ is analytically possible if $B_c(z) = -B_p(z)$. The convergence of $B_c(z) \to -B_p(z)$ and $\varepsilon(t) \to 0$ is not a problem if one applies the filtered-x LMS algorithm to Fig. 3. This is, in fact, an important advantage of the new controller. For other ANC systems, $E\{\varepsilon^2(t)\} = 0$ is analytically impossible by the application of a FIR filter. As shown in Eqs. (2) and (3), $C_{id}(z)$ and $G_{id}(z)$ are IIR filters even if all path models are FIR filters. Most adaptive ANC systems use adaptive FIR filter $C(z)$ or $G(z)$ to approximate IIR filter $C_{id}(z)$ or $G_{id}(z)$. Even if $R(z)$, $S(z)$ and $F(z)$ are available accurately, it is impossible to achieve $E\{\varepsilon^2(t)\} = 0$ by those methods because a FIR filter cannot match an IIR filter exactly.

The proposed method makes better use of the available knowledge due to its new configuration represented by the gray-box in Fig. 3. The ANC controller consists of different internal blocks. Some of the internal blocks can be derived from $S(z)$ or $F(z)$. Only part of the controller, $B_c(z)$, is made adaptive. The separate treatment of the ANC controller makes it possible to achieve $E\{\varepsilon^2(t)\} = 0$ if $B_c(z)$ converges to FIR filter $-B_p(z)$.

In the derivations of this section, it is temporarily assumed that $S(z)$ and $R(z)$ are MP. The ideal controller transfer functions $C_{id}(z)$ or $G_{id}(z)$ are stable under such an assumption. The focus is the separate treatment of internal blocks of the ANC controller. Another obstacle to objective $E\{\varepsilon^2(t)\} = 0$ is the NMP zeros in $S(z)$ or $R(z)$. The ideal ANC controller is unstable when either $S(z)$ or $R(z)$ is NMP. That is the focus of the next section.

3. Dealing with NMP paths

Attention is now directed to the case of a NMP secondary path $S(z)$ if the error sensor is not collocated with the secondary speaker, though it is reasonable to assume a MP $R(z)$ when the reference sensor is collocated with or close to the primary source. In case $R(z)$ is NMP, similar treatments on $S(z)$ are also applicable to $R(z)$ since $S(z)R(z)$ is equivalent to a single model for SISO systems.

For a SISO ANC system with a NMP secondary path, it is possible to achieve optimal performance in the minimum H_2 norm sense based on the knowledge of $P(z)$, $S(z)$ and direct availability of primary noise signal $n(z)$ [14]. In case $P(z)$ and $n(z)$ are not available, a method is proposed here to implement an adaptive H_2 controller. The new ANC structure is given in the gray-box of Fig. 4. The IIR filter $B_s^{-1}(z)$ in Fig. 3 is unstable if $B_s(z)$ is NMP. It is replaced by a stable $\tilde{B}_s^{-1}(z)$ in Fig. 4. This is possible if one mirrors the NMP roots of $B_s(z)$ into the unit circle to obtain $\tilde{B}_s(z)$.

The use of $\tilde{B}_s^{-1}(z)$ is related to the H_2 controller design theory. One way to design an H_2 controller is to factorize $S(z) = V_a(z)V_m(z)$, where $V_a(z)$ is an all-pass filter and $V_m(z)$ is a MP filter. Let $B_s(z) = B_n(z)B_m(z)$ where $B_n(z)$ and $B_m(z)$ contain the NMP and MP roots of $B_s(z)$ respectively. If the degree of $B_n(z) = \sum_{i=0}^{d_n} b_{ni}z^{-i}$ is d_n, then $\tilde{B}_n(z) = \sum_{i=0}^{d_n} b_{n(d_n-i)}z^{-i}$ can be obtained by using coefficients of $B_n(z)$ in the reversed order. If the roots of $B_n(z)$ are $\{r_i\}$, then the roots of $\tilde{B}_n(z)$ will be $\{1/r_i\}$ [15]. Since $|r_i|>1$ for all roots of $B_n(z)$, $\tilde{B}_n(z)$ is stable. One may then write

$$S(z) = \frac{B_s(z)}{A(z)} = \frac{B_n(z)}{\tilde{B}_n(z)}\frac{\tilde{B}_n(z)B_m(z)}{A(z)} = \frac{B_n(z)}{\tilde{B}_n(z)}\frac{\tilde{B}_s(z)}{A(z)}. \tag{9}$$

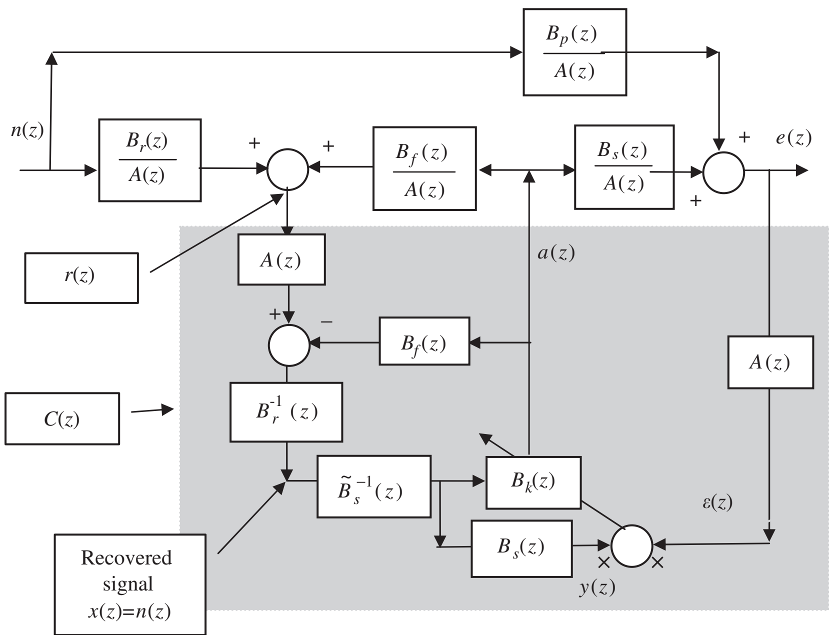

Fig. 4. Block diagram of the proposed ANC (adaptive with NMP secondary path).

It can be shown $\left|\tilde{B}_n(e^{j\omega})\right| = \left|e^{-d_n j\omega} B_n(e^{-j\omega})\right| = \left|B_n(e^{j\omega})\right|$ for all ω [15], therefore $(B_n(z))/(\tilde{B}_n(z))$ is a stable all-pass filter. A possible factorization of $S(z) = V_a(z)V_m(z)$ would be

$$V_a(z) = \frac{B_n(z)}{\tilde{B}_n(z)} \quad \text{and} \quad V_m(z) = \frac{\tilde{B}_s(z)}{A(z)} \tag{10}$$

for the design of an H_2 ANC controller.

If $R(z) = 1$, $n(z)$ is broadband white noise, $P(z)$ and $n(z)$ were available, then an optimal controller $C_{opt}(z)$ could be sought to minimize $||[P(z) + S(z)C_{opt}(z)]n(z)||_2$. This could be done by the minimization of

$$\left\|P + SC_{opt}\right\|_2 = \left\|V_a(z)\right\|_2 \left\|V_a^{-1}P + V_m C_{opt}\right\|_2 = \left\|V_a^{-1}P + V_m C_{opt}\right\|_2, \tag{11}$$

where $||V_a(z)||_2 = 1$ since it is an all-pass filter. One may apply partial fraction expansion to write

$$V_a^{-1}(z)P(z) = \frac{\tilde{B}_n(z)}{B_n(z)}\frac{B_p(z)}{A(z)} = \frac{K_u(z)}{B_n(z)} + \frac{K_s(z)}{A(z)}, \tag{12}$$

where FIR filters $K_u(z)$ and $K_s(z)$ are determined by the coefficients of $B_p(z)$. The two parts in the right-hand side of Eq. (12) are orthogonal to each other in the H_2 norm sense. Since $(K_u(z))/(B_n(z))$ is the unstable part of $V_a^{-1}(z)P(z)$, it cannot be cancelled by any stable feedforward controller. The best control result, in the minimum H_2 norm sense, is the cancellation of the stable part of $V_a^{-1}(z)P(z)$ by an optimal controller in the form of

$$C_{opt}(z) = -V_m^{-1}(z)\frac{K_s(z)}{A(z)} = -\frac{A(z)}{\tilde{B}_s(z)}\frac{K_s(z)}{A(z)} = -\frac{K_s(z)}{\tilde{B}_s(z)}. \tag{13}$$

By substituting Eqs. (12) and (13) into Eq. (11), one minimizes $\left\|P + SC_{opt}\right\|_2 = \left\|K_u/B_n\right\|_2$ in the H_2 norm sense. From this point of view, the best controller for a broadband ANC system with a NMP secondary path is an IIR filter $C_{opt}(z)$. It remains an IIR filter even if $S(z) = B_s(z)$ becomes a FIR filter when $A(z) = 1$. One can only degrade $\|P + SC\|_2 > \left\|K_u/B_n\right\|_2$ by replacing $C_{opt}(z)$ with any other ANC controllers.

A problem with available ANC systems is the use of an adaptive FIR filter $C(z)$ to approximate $C_{opt}(z)$ when $P(z)$ and $n(z)$ are not available. This leaves room for improvement since a FIR filter can never match an IIR filter exactly. Any mismatch between FIR filter $C(z)$ and IIR filter $C_{opt}(z)$ can only degrade $\|P + SC\|_2 > \left\|K_u/B_n\right\|_2$. The proposed ANC controller, represented by the gray-box of Fig. 4, is applicable to improve ANC performance in this direction. Signal-processing operations inside the new controller are described by Eqs. (5), (14)–(16). Since the measured reference signal $r(z)$ contains the acoustical feedback, $C_{opt}(z)$ cannot be implemented directly. Eq. (5) must be used to cancel the acoustic feedback and recover $x(z) = n(z)$, hence the similarity between Figs. 3 and 4. The actuation signal in Fig. 4 is synthesized by

$$a(z) = \frac{B_k(z)}{\tilde{B}_s(z)}n(z). \tag{14}$$

Since $|[P(z) + S(z)C_{opt}(z)]n(z)|$ is the best achievable result in the H_2 norm sense, the optimal actuation signal must be $a(z) = C_{opt}(z)n(z)$. This means $B_k(z)$ should converge to $-K_s(z)$ by comparing Eqs. (13) and (14). Therefore, the new ANC controller requires the convergence of

$B_k(z)$ to FIR filter $-K_s(z)$ for best performance in the minimum H_2 norm sense when the secondary path is NMP.

Since $P(z)$ is not available, $K_s(z)$ cannot be obtained directly. Its degree, however, is predictable if the degree of $B_p(z)$ is predictable. With a predicted degree, $B_k(z)$ is adapted by the application of the filtered-x LMS algorithm. Similar to the derivation of Eq. (7), one may express the error signal in Fig. 4 as

$$\begin{aligned} \varepsilon(z) &= B_p(z)n(z) + B_s(z)a(z) \\ &= \left[B_p(z) + B_k(z)\frac{B_s(z)}{\tilde{B}_s(z)}\right]n(z) \\ &= B_p(z)n(z) + B_k(z)y(z), \end{aligned} \tag{15}$$

where

$$y(z) = \frac{B_s(z)}{\tilde{B}_s(z)}x(z).$$

Let $d(t)$ represent the time-domain signal of $d(z) = B_p(z)n(z)$. The time-domain version of $\varepsilon(z)$, given by

$$\varepsilon(t) = d(t) + \sum_{i=0}^{m} b_{ki}y(t-i),$$

may to used to derive

$$\frac{\partial}{\partial b_{ki}}E\{\varepsilon^2(t)\} = 2E\{\varepsilon(t)y(t-i)\}. \tag{16}$$

These are elements of the gradient vector for the adaptive filter $B_k(z)$ in Fig. 4. The convergence of $B_k(z) \to -K_s(z)$ is possible by the application of the filtered-x LMS algorithm.

The stability of the new controller can be established by showing that all internal signals $x(z)$, $y(z)$ and $a(z)$ are bounded-in-bounded-out (BIBO) stable. The analytical expression $x(z)$ is given by Eq. (5), where $a(z)$ is cancelled out and $B_r(z)$ is MP by assumption. Therefore $x(z) = n(z)$ is BIBO stable. In case $B_r(z)$ is NMP, its treatment is similar to the treatment of $B_s(z)$. Next,

$$y(z) = \frac{B_s(z)}{\tilde{B}_s(z)}x(z)$$

is also BIBO stable since $\tilde{B}_s(z)$ is stable. Adaptive coefficients of $B_k(z)$ are determined by the filtered-x LMS algorithm with a BIBO gradient given by Eq. (16). Therefore coefficients of $B_k(z)$ are uniformly bounded as long as the adaptation step size is sufficiently small. The stability of $a(z)$ depends on Eq. (14), which is BIBO stable because $\tilde{B}_s(z)$ is stable and coefficients of $B_k(z)$ are uniformly bounded. The use of $\tilde{B}_s(z)$ plays an important part in the stability of the ANC controller. Otherwise, if $B_s(z)$ was not replaced by $\tilde{B}_s(z)$, internal signals $y(z)$ and $a(z)$ would be unstable when the ANC system has a NMP secondary path.

4. Experimental verification

The proposed method was tested experimentally in a duct with a length of 2 m and a cross-section of $11 \times 15\,\text{cm}^2$. The experimental setup is shown in Fig. 5. The primary source was placed at the right end of the duct. The secondary source was 1 m away from the primary source. These are 4 in speakers with 800 mw capacity. The reference and error sensors (B&K 4130 microphones) were placed, respectively, at the right- and-left-hand sides of the secondary source. The ANC was implemented in a dSPACE 1103 board with a sampling frequency 2.5 kHz. The actuator output signals are in the range of ± 5 V, which were amplified by a two-channel power amplifier to drive the primary and secondary speakers. Analog signals were filtered by anti-alias filters with cut-off frequencies set to 1000 Hz. Noise suppression performance was tested in a range of 80–1000 Hz, which is limited by the geometric size of the speakers and the cut-off frequency of anti-alias filters.

The primary source $n(z)$ was pseudo-random noise generated by the dS1103, but the reference signal was measured by a sensor placed close to the primary speaker. Different holes were drilled in the upstream segment to test the locations of reference sensor, which could affect the coherence between the recovered signal $x(z)$ and the primary source $n(z)$. For the proposed approach, $x(z)$ is recovered by Eq. (5) with $B_r(z)$ as the denominator. A highly coherent $x(z) = n(z)$ requires a MP $B_r(z)$, which is possible if the reference sensor is sufficiently close to the primary source. This approach is more realistic than other methods that assume $R(z) = 1$.

The power spectral density (PSD) of $e(z)$ is divided by the PSD of $n(z)$ to be the normalized PSD and then plotted in Fig. 6 for three different cases. In Case 1, the normalized PSD of $e(z)$ was obtained without ANC. It is equivalent to the magnitude responses of $P(z)$ with $G(z) = 0$ in

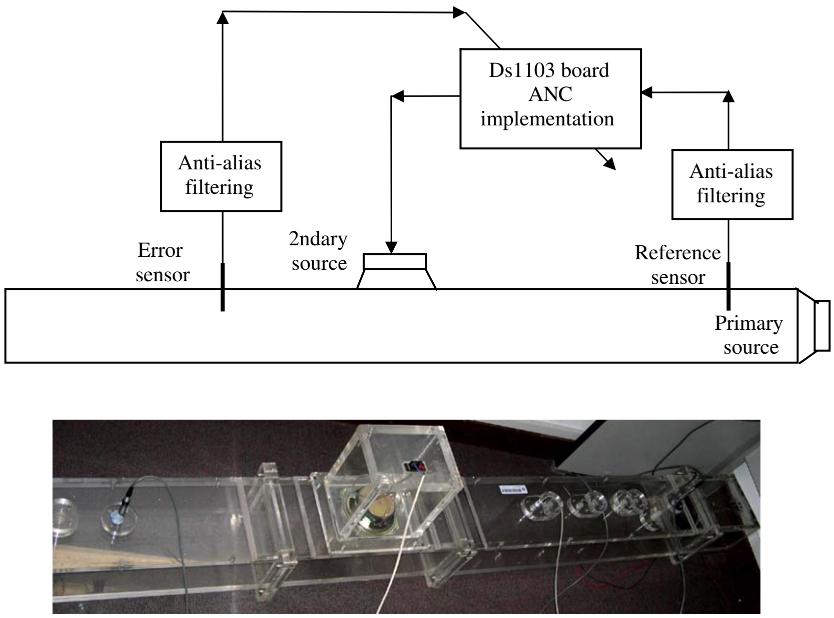

Fig. 5. Experiment setup (schematic and photograph).

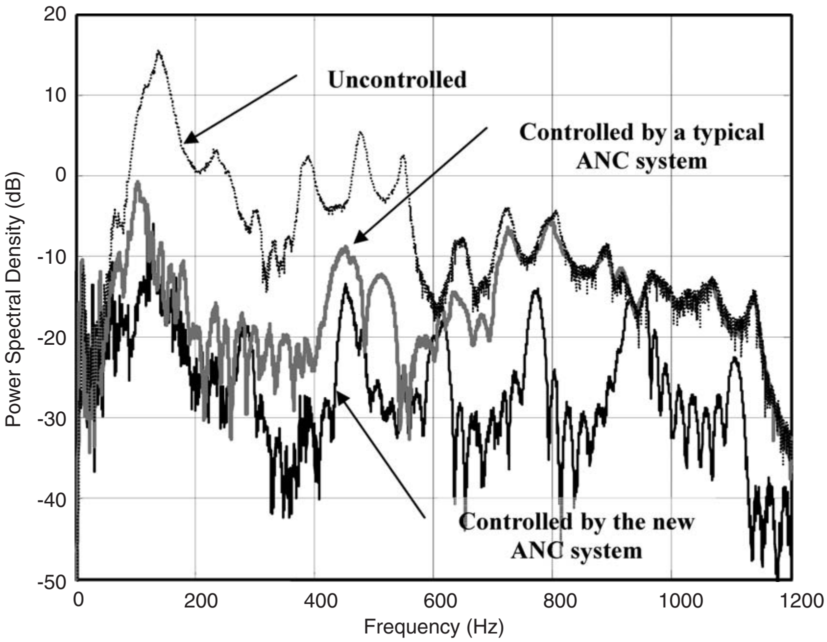

Fig. 6. Normalized PSD of $e(z)$, with ANC off (dashed), typical ANC (gray), and new ANC (black), respectively.

Eq. (1). The corresponding data are plotted in Fig. 6 as the dashed curve. It serves as the reference for the comparison between a typical ANC controller and the proposed one.

In Case 2, a typical ANC controller was implemented using the block diagram structure of Fig. 1. Path transfer functions $F(z)$, $S(z)$ and $R(z)$ were approximated by FIR filters with 256 coefficients. The ANC system attempted to use a 256-coefficient FIR filter $C(z)$ to match IIR filter $C_{\rm opt}(z)$. This is an existing problem discussed in Section 3. Although $C(z)$ converged as expected, it was impossible to match $C_{\rm opt}(z)$ exactly, and the mismatch would only degrade $\|P+SC\|_2 > \|K_u/B_n\|_2$ of the noise path. For Case 2, the normalized PSD of $e(z)$ is plotted in Fig. 6, as the gray curve.

Case 3 needs more detailed explanations because the proposed method was tested in this case. The equation error method [16] was applied to identify

$$F(z) = \frac{B_f(z)}{A(z)}, \quad S(z) = \frac{B_s(z)}{A(z)} \quad \text{and} \quad R(z) = \frac{B_r(z)}{A(z)}$$

where the degrees of $A(z)$, $B_f(z)$, $B_s(z)$ and $B_r(z)$ were 80. Magnitude responses of the secondary path and its IIR model are plotted in Fig. 7 as the gray and black curves, respectively. The non-parametric magnitude response of $S(z)$ was computed as the PSD of $e(z)$ normalized by the PSD of $n(z)$, when $n(z)$ was connected to the secondary source. The identification of $S(z)$ is very accurate, since the two curves in Fig. 7 almost overlap exactly in the frequency range of interests. The non-parametric magnitude response of $P(z)$ is actually the normalized PSD shown in Fig. 6 as the dashed curve. The path model was not identified since this may not be possible in real applications. Only the IIR model of $S(z) = B_s(z)/A(z)$ was required in the experiment. The NMP

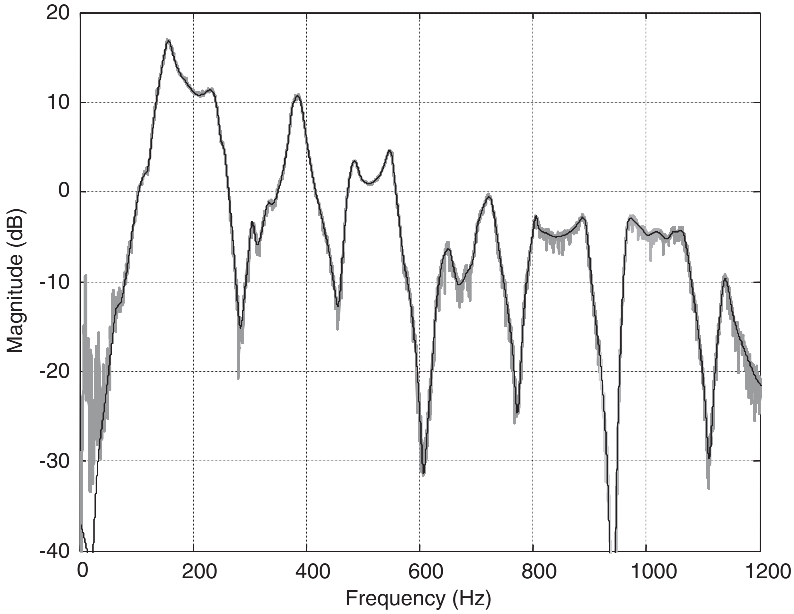

Fig. 7. Magnitude responses of the secondary path (gray) and its IIR model (black).

zeros of $B_s(z)$ were mirrored into the unit circle to obtain $\tilde{B}_s(z)$. The new ANC controller was then implemented using the block diagram of Fig. 4.

Experimental data were collected to obtain the normalized PSD of $e(z)$ when the new ANC was active. These data are plotted in Fig. 6 as the black curve for Case 3. The new controller attenuates noise more effectively in the frequency range of interest. Its control performance is very close to the predicted control performance as shown in Fig. 8, where the thick gray curve represents the performance of the proposed controller and the thin black curve represents the predicted control performance. The mean square errors are plotted in Fig. 9, for the typical ANC (thick gray curve) and the new ANC systems (thin black curve), respectively. The new ANC system achieves approximately 7 dB improvement in the mean square error over the typical one. The cost of improvement is the offline computations for $\tilde{B}_s(z)$ and more online computations during each sampling interval. A typical adaptive ANC controller requires online filtering of $F(z)$ and $S(z)$ to cancel the acoustical feedback and obtain the filtered-x signal. This is roughly the computation load of $B_f(z)$ and $B_s(z)$ in the dashed-box of Fig. 4. The additional online computations are filter operations of $A(z)$ and $\tilde{B}_s^{-1}(z)B_r^{-1}(z)$. These are required to compute the gradient ∇_k, whose elements are given by Eq. (16).

Let $\mathbf{w}_k$ denote the weights of an adaptive FIR filter, the operation of an LMS may be expressed as $\mathbf{w}_{k+1} = \mathbf{w}_k - \mu\nabla_k$, where μ is the step size. The increased load of ∇_k is not a problem for most DSP chips when the sampling rate is 2.5 kHz. As long as ∇_k is updated within each sampling interval, the convergence rate of $\mathbf{w}_{k+1} = \mathbf{w}_k - \mu\nabla_k$ will not be affected if μ remains the same. In the experiment, the value of μ was determined by trial and error and set to $\mu = 0.01$ for both the typical ANC controller and the proposed one. Both ANC controllers converged at roughly the same speed. The adaptive $B_k(z)$ attempted to match a FIR filter $K_s(z)$ for best performance in

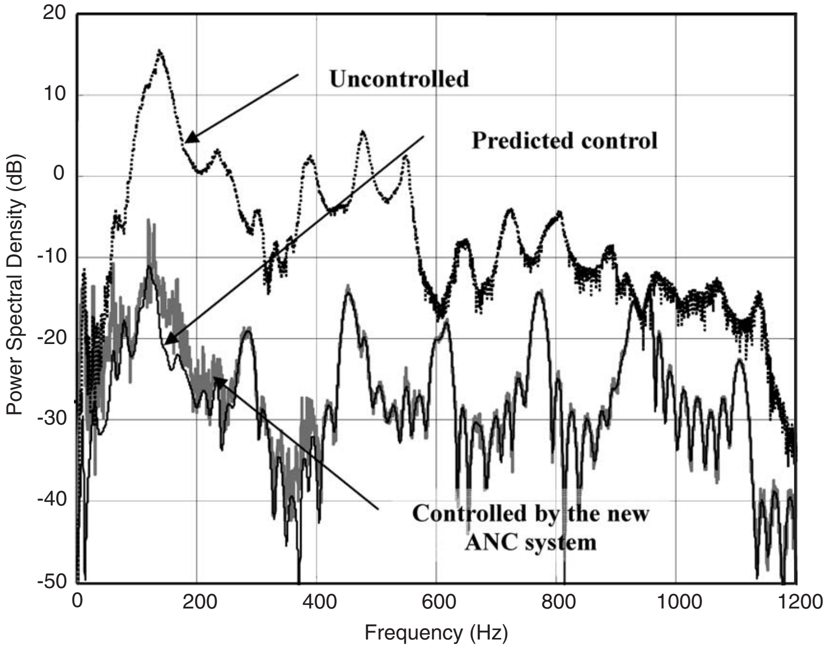

Fig. 8. Normalized PSD of $e(z)$ with ANC off (dashed), predicted control (thin black), and new ANC (thick gray), respectively.

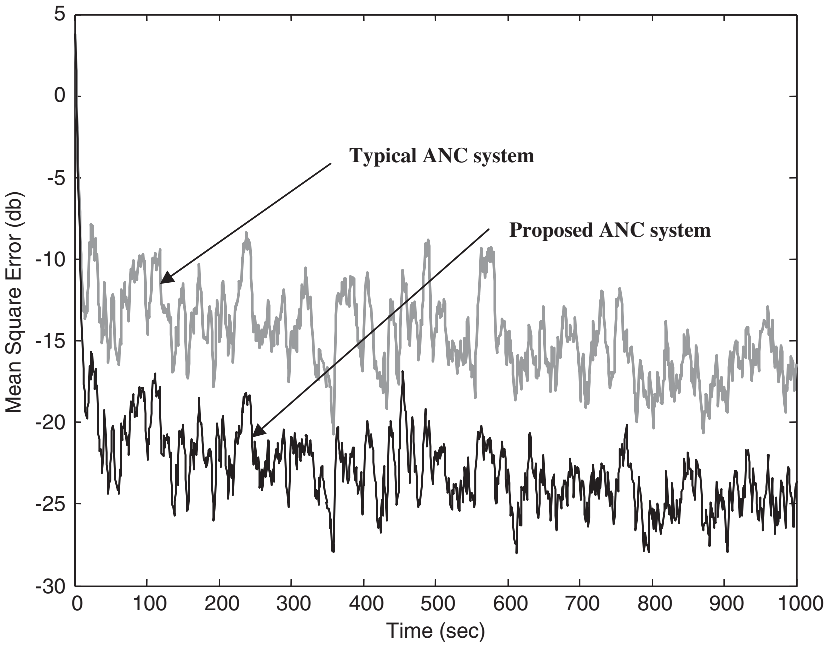

Fig. 9. Mean square error of the typical ANC system (thick gray), and new ANC system (thin black).

the minimum H_2 norm sense. This was similar to the typical ANC controller whose $C(z)$ attempted to match an IIR filter $C_{opt}(z)$ under a same conditions. The new controller was observed as stable as a typical ANC controller.

5. Conclusion

In this study, the ideal ANC is defined as one that drives the error signal $e(z)$ to zero when the primary source $n(z)$ is broadband white noise. Under the same conditions, the best ANC is one that minimizes the H_2 norm of the noise path. It is shown analytically that the ideal and best ANC controllers are IIR filters even when all path models of the noise field are FIR filters.

When the secondary paths are NMP, which is a frequently encountered situation in ANC systems, it is impossible to drive $e(z) = 0$. Only the best ANC controller is practically applicable, which is an IIR filter $C_{opt}(z)$ given in Eq. (13). Many available ANC systems use an adaptive FIR filter $C(z)$ to match IIR filter $C_{opt}(z)$. Any mismatch between $C(z)$ and $C_{opt}(z)$ only degrades the ANC performance in the H_2 norm sense.

The problem can be solved by the proposed ANC system that makes better use of the path models. By the proper design of the ANC structure, only a sub-block of the controller is made adaptive. The entire ANC controller will match $C_{opt}(z)$ for the best performance in the minimum H_2 norm sense. When the secondary path is MP, the new ANC controller will drive $e(z) = 0$ if its adaptive block converges to FIR filter $-B_p(z)$. Experimental results are presented to verify the analytical results.

Acknowledgement

The work described in this paper was substantially supported by a grant from the Research Grants Council of the Hong Kong Special Administration Region (Project No. PolyU 5175/01E).

References

[1] P.A. Nelson, S.J. Elliott, *Active Control of Sound*, Academic Press, London, 1992.
[2] C.H. Hansen, S.D. Snyder, *Active Control of Noise and Vibration*, E and FN Spon, London, 1997.
[3] T. Meurers, S.M. Veres, S.J. Elliot, Frequency selective feedback for active noise control, *IEEE Control Systems Magazine* 22 (2002) 32–41.
[4] J. Romeu, S. Jimenez, R. Capdevila, N. Diaz, Reduction of noise transmission through an aperture using active feedforward noise control, *Journal of Acoustical Society of America* 111 (2002) 41–49.
[5] S.M. Kuo, Kong. Xuan, W.S. Gan, Applications of adaptive feedback active noise control system, *IEEE Transactions on Control Systems Technology* 11 (2) (2003) 216–220.
[6] PL.J. Eriksson, Development of the filtered-U algorithm for active noise control, *Journal of Acoustical Society of America* 89 (1991) 257–265.
[7] R. Fraanje, M. Verhaegen, N. Doelman, Convergence analysis of the filtered-U LMS algorithm for active noise control in case perfect cancellation is not possible, *Signal Processing* 83 (2003) 1239–1246.
[8] D.H. Crawford, R.W. Stewart, Adaptive IIR filtered-v algorithms for active noise control, *Journal of Acoustical Society of America* 101 (1997) 2097–2103.

[9] J. Liu, C. Shen, X. Qiu, B. Xu, Lattice form adaptive infinite impulse response filtering algorithm for active noise control, *Journal of Acoustical Society of America* 113 (2003) 327–335.
[10] A.P. Liavas, P.A. Regalia, Acoustic echo cancellation: do IIR models offer better modeling capabilities than FIR counterparts?, *IEEE Transactions on Signal Processing* 46 (1998) 2499–2504.
[11] J.S. Vipperman, R.A. Burdisso, Adaptive feedforward control of non-minimum phase structural systems, *Journal of Sound and Vibration* 183 (3) (1995) 369–382.
[12] J. Yuan, Relaxed condition for 'perfect' cancellation of broadband noise in 3D enclosures, *Journal of Acoustical Society of America* 107 (2000) 3235–3244.
[13] S. Liu, J. Yuan, K.-Y. Fung, Robust active control of broadband noise in finite ducts, *Journal of Acoustical Society of America* 111 (2002) 2727–2733.
[14] M.-R. Bai, H.-P. Chen, Development of a feedforward active control system by using the H_2 and H_∞ model matching principle, *Journal of Sound and Vibration* 201 (2) (1997) 189–204.
[15] P.A. Regalia, *Adaptive IIR Filtering in Signal Processing and Control*, Dekker, New York, 1995.
[16] G.C. Goodwin, K.S. Sin, *Adaptive Filtering, Prediction and Control*, Prentice-Hall, Englewood Cliffs, NJ, 1984.